

Grazing-incidence spectrometer for soft x-ray and extreme ultraviolet spectroscopy on the National Spherical Torus Experiment

P. Beiersdorfer

Lawrence Livermore National Laboratory, Livermore, California 94550

M. Bitter and L. Roquemore

Princeton Plasma Physics Laboratory, Princeton, New Jersey 08543

J. K. Lepson

University of California, Berkeley, California 94720

M.-F. Cu

Stanford University, Palo Alto, California 94305

(Received 1 May 2006; presented on 10 May 2006; accepted 31 May 2006; published online 22 September 2006)

A compact grazing-incidence spectrometer has been implemented on the National Spherical Torus Experiment for spectral measurements in the 6–65 Å spectral region. The spectrometer employed a 2400ℓ/mm grating designed for flat-field focusing and a cryogenically cooled charge-coupled device camera for readout. The instrument was tested by recording the *K*-shell lines of boron, carbon, nitrogen, and oxygen, as well the *L*-shell lines from argon, iron, and nickel that fall into this spectral band. The observed linewidth was about 0.1 Å, which corresponds to a resolving power of 400 for the *C V* lines. A temporal resolution as fast as 50 ms was obtained. © 2006 American Institute of Physics. [DOI: 10.1063/1.2220478]

I. INTRODUCTION

Spectroscopic measurements of soft x ray and extreme ultraviolet radiation have been established as excellent ways of monitoring the concentration of impurities in hot plasma,¹ because a wealth of lines from many ionization stages of numerous elements falls into this wavelength band. As a result, instrumentation to monitor this wavelength band has been commonly implemented on magnetic fusion devices.^{2–8} Many of these instruments cover a broad spectral region in order to survey as many elements and ionization stages as possible. For similar reasons, the soft x ray and extreme ultraviolet wavelength region of interests to astrophysics, where such measurements provide values for elemental abundances and charge balances. Additional interest derives from the fact that many lines in this wavelength region are sensitive to changes in the electron density and can be used as diagnostics of the plasma conditions.

In the following we describe a compact grazing-incidence spectrometer for use on the National Spherical Torus Experiment (NSTX). The instrument has been set up for monitoring line emission in the 6–65 Å region. In particular, we are interested in the emission from hydrogenlike and heliumlike boron, carbon, nitrogen, and oxygen, as well as the emission from lithiumlike through neonlike ions of the transition metals, i.e., Ti, V, Cr, Mn, Fe, Co, Ni, and Cu.

Because boronization and the use of carbon limiters diminish the possibility of metal ions entering the discharge during normal operation,^{9,10} observations of lines from metal ions in the spectra are indicators of wear on the protective coatings. Examples would be copper from the antennae used in radio-frequency (rf) heating or titanium from the titanium

carbide surface coating of the Faraday shields of the high-harmonic fast wave (HHFW) rf heating system. Observation of nitrogen lines may indicate an air leak or plasma touching limiters on the rf system, which are made of boron nitride. Alternatively, the lack of boron lines in these spectra can indicate that the effect of boronization has worn off.

The spectral range of the present instrument complements that of the high-resolution vacuum crystal spectrometer used for spectral measurements in the soft x-ray regime between about 7 and 24 Å, which has a resolving power above 1000,^{6,11} and the low-resolution ($\lambda/\Delta\lambda \approx 50$ –400) survey, poor resolution, extended domain (SPRED) instrument for measurements in the 100–1100 Å region.^{2,4} The new spectrometer has a resolving power of about 150–500.

Because the electron temperature and density of NSTX plasmas are well known from Thomson scattering measurements,⁹ the instrument allows us to calibrate spectral lines ratios useful as plasma diagnostics. Tokamak plasmas have played an important role in testing atomic physics and providing well calibrated diagnostics for astrophysics.^{12–16} The new instrument illustrates this possibility by studying the spectra from *L*-shell argon ions, whereby argon was deliberately introduced into NSTX for this purpose. The spectra of *L*-shell argon ions relevant to x-ray astronomy have been measured in detail before at the electron beam ion trap facility at the University of California Lawrence Livermore National Laboratory.¹⁷ The NSTX measurements, however, provide spectral emission at considerably higher electron densities ($>10^{13}$ cm⁻³ vs 10^{11} cm⁻³ at the electron beam ion trap), i.e., in a density regime needed to calibrate, for example, diagnostics of high-density stellar flare plasmas.

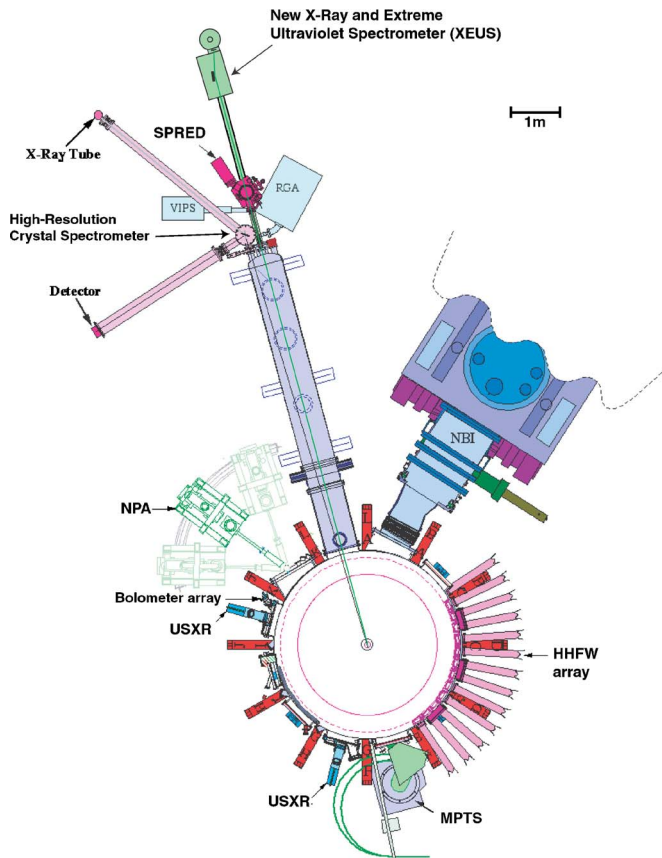


FIG. 1. Diagnostic layout on the NSTX tokamak showing the location of the new grazing-incidence spectrometer at the end of the pump duct.

II. SPECTROMETER DESIGN

The new x-ray and extreme ultraviolet spectrometer (XEUS) is similar to that employed earlier at the Livermore electron beam ion trap facility.¹⁸ It employs a variable line spacing grating mounted on a rotary table [average line spacing of $2400\ell/\text{mm}$ (Ref. 19)]. The Hitachi grating affords flat-field focusing in the 6–100 Å range with a focal distance of about 23 cm. The angle of incidence is 1.3° . The blaze angle is 15 Å.

The XEUS instrument is located at the end of the NSTX pump duct, and thus is about 10 m away from the vacuum vessel. Its line of sight follows a radial line to the center stack of the tokamak within the horizontal midplane of the plasma. A layout of the instrument on NSTX is shown in Fig. 1.

Because NSTX plasmas are extended sources, we employ either a 30 or 100 μm entrance slit in order to provide a linewidth commensurate with the 25 μm pixel size of the liquid nitrogen cooled Photometrics charge couple device (CCD) camera used for spectral recording. The 1 in. \times 1 in. detector allows us to monitor the region between 10 and 65 Å in a single setting. Adjustments in the camera position are possible to access shorter wavelength regions, including the location of the zero-order reflection.

A shutter before the entrance slit is used to provide time resolution. The shutter can be opened and closed within about 30 ms. Periods of interest can be selected by opening and closing the shutter at the appropriate times during a NSTX discharge. The shortest period that provided sufficient

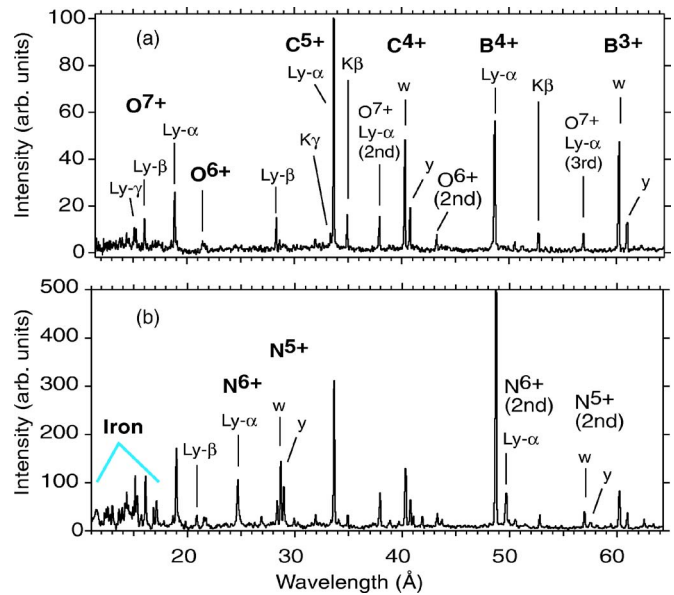


FIG. 2. *K*-shell emission features observed with XEUS during typical NSTX discharges. The ion corresponding to a given line observed in first order reflection is indicated in boldface type. Lyman α , β , and γ denote the $2p \rightarrow 1s$, $3p \rightarrow 1s$, and $4p \rightarrow 1s$ transitions in hydrogenlike ions, respectively. w , $K\beta$, and $K\gamma$ denote the $1s2p\ ^1P_1 \rightarrow 1s^2\ ^1S_1$, $1s3p\ ^1P_1 \rightarrow 1s^2\ ^1S_1$, and $1s4p\ ^1P_1 \rightarrow 1s^2\ ^1S_1$ transitions in heliumlike ions, respectively. y denotes the $1s2p\ ^3P_1 \rightarrow 1s^2\ ^1S_1$ transition. (a) Ohmically heated helium discharge (shot 117083); (b) neutral-beam heated discharge (shot 117927). Note the added emission from hydrogenlike and heliumlike nitrogen as well as from high charge states of iron.

signal was 50 ms, i.e., keeping the shutter open for 20 ms in addition to the 30 ms opening and closing times.

At present, no shielding is employed against hard x rays. These are not a problem during Ohmic or rf-heated discharges. However, hard x rays generated during neutral beam conditioning or neutral beam heating penetrate the detector housing and increase the overall background of the observed spectra, albeit not enough to mask the emission of the strong *K*-shell lines of B, C, and O.

III. PERFORMANCE

A typical spectrum obtained with the new spectrometer is shown in Fig. 2(a). It was taken during the Ohmic heating phase ($T=320\text{--}750$ ms) of a lower single null helium plasma (NSTX shot 117084). The spectral emission is almost exclusively comprised of the *K*-shell lines from hydrogenlike and heliumlike boron, carbon, and oxygen. Of interest is the emission from heliumlike O^{6+} , which is weak compared to that of H-like O^{7+} . This is surprising, given that the emission of the heliumlike B and C is strong. One explanation is that the grating is less sensitive at near 21 Å compared to its sensitivity near 19 Å, i.e., the position of the Lyman- α line of O^{7+} . Another is that there are relatively fewer O^{6+} ions in the plasma than there are B^{3+} or C^{4+} ions. While this is unlikely, this possibility needs to be checked with charge balance calculations.

Note that no nitrogen is seen. This is typical for NSTX discharges. Strong *K*-shell lines from hydrogenlike and heliumlike nitrogen have been seen in a few pellet injection or rf-heated plasmas,¹⁰ as illustrated in Fig. 2(b).

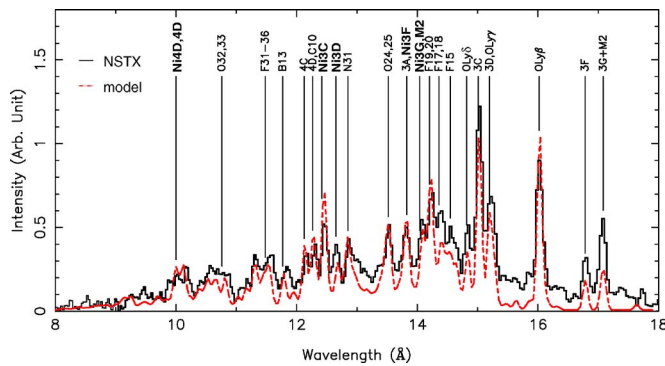


FIG. 3. Expanded view of the $n=3 \rightarrow n=2$ emission of iron recorded during a discharge heated with a 6 MW neutral beam (shot 114459). The spectrum was fitted with an emission model constructed with the FLEXIBLE ATOMIC CODE (Ref. 20). All features are from iron, except those from nickel (labeled in boldface type) and the oxygen Lyman β , γ , and δ lines.

We note that essentially no lines from metal impurities are seen in the spectrum in Fig. 2(a). Lines from L -shell iron ions, however, can be seen under different NSTX run conditions, especially when the plasma is allowed to expand toward the outer wall, as illustrated in Fig. 2(b). A typical spectrum of the $n=3 \rightarrow n=2$ lines of lithiumlike through neonlike iron, which falls into the 8–17 Å region, is shown in Fig. 3. The spectrum was fitted with a spectral model produced by the FLEXIBLE ATOMIC CODE,²⁰ and good agreement was found. Three major features, however, could not be fitted with the iron model alone. These were determined to be $n=3 \rightarrow n=2$ lines of nickel.

In Fig. 4 we present a spectrum recorded after an argon puff into NSTX. The two most prominent lines are $3s \rightarrow 2p$ transitions of Ar^{8+} . We note the absence of the dipole-forbidden magnetic quadrupole (M2) transition $1s^2 2s^2 2p_{3/2}^5 3s_{1/2}^3 P_2 \rightarrow 1s^2 2s^2 2p^6 {}^1S_0$. This line is quenched at the electron densities found in NSTX, in accordance with predictions of its sensitivity on electron density.²¹

From the observed spectra we measure a linewidth of roughly a little over 0.10 Å, as summarized in Table I. From this we infer a resolving power of about 150 near 15 Å, of 350 near 34 Å, and of more than 400 above 50 Å. This is comparable to the Schwob-Fraenkel instrument [soft x-ray

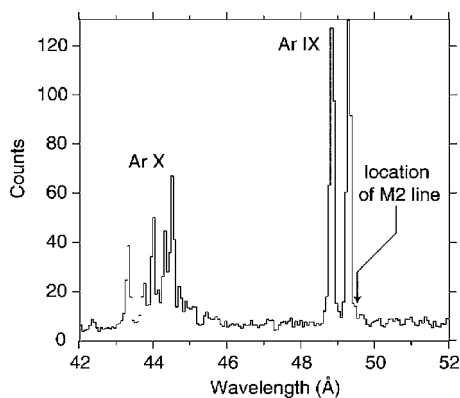


FIG. 4. Argon emission recorded during Ohmically heated discharges (sum of shots 117313 and 117320). The arrow points to the location of the forbidden magnetic quadrupole transition in Ar IX, which is collisionally quenched at the line-averaged density $n_e (\approx 3 \times 10^{13} \text{ cm}^{-3})$ in this discharge. The B^{4+} Lyman α line was subtracted from the spectrum for clarity.

TABLE I. Measured linewidths and associated instrumental resolving power using a 30 μm slit.

Line	Wavelength (Å)	Linewidth (Å)	$\lambda/\Delta\lambda$
O^{7+} Ly- γ	15.14	0.10	151
O^{7+} Ly- β	16.11	0.10	161
O^{7+} Ly- α	19.00	0.13	146
C^{5+} Ly- α	33.73	0.09	387
C^{4+} w	40.31	0.10	403
B^{4+} Ly- α	48.77	0.14	356
O^{7+} Ly- α	56.97 ^a	0.11	540
B^{3+} w	60.23	0.13	465

^aThird order.

multichannel spectrometer (SOXMO5)] operated with a 600 ℓ/mm grating and a 10 μm slit. The resolution of our instrument could be improved by about a factor of 3 by using a slit of similar width, at which point the resolving power would be limited by the 25 μm pixel size of the CCD detector.

ACKNOWLEDGMENTS

This work was performed under the auspices of the Department of Energy by the University of California Lawrence Livermore National Laboratory under Contract No. W-7405-ENG-48 and supported by the Office of Fusion Energy Basic and Applied Plasma Science Initiative.

- ¹C. D. Michelis and M. Mattioli, Rep. Prog. Phys. **47**, 1233 (1984).
- ²R. J. Fonck, A. T. Ramsey, and R. V. Yelle, Appl. Opt. **21**, 2115 (1982).
- ³W. L. Hodge, B. C. Stratton, and H. W. Moos, Rev. Sci. Instrum. **55**, 16 (1984).
- ⁴B. C. Stratton, R. J. Fonck, K. Ida, K. P. Jaehrig, and A. T. Ramsey, Rev. Sci. Instrum. **57**, 2043 (1986).
- ⁵J. L. Schwob, A. W. Wouters, S. Suckewer, and M. Finkenthal, Rev. Sci. Instrum. **58**, 1601 (1987).
- ⁶P. Beiersdorfer, S. von Goeler, M. Bitter, K. W. Hill, R. A. Hulse, and R. S. Walling, Rev. Sci. Instrum. **60**, 895 (1989).
- ⁷A. R. Field, J. Fink, R. Dux, G. Fussmann, U. Wenzel, and U. Schumacher, Rev. Sci. Instrum. **66**, 5433 (1995).
- ⁸W. Biel, G. Bertschinger, R. Burhenn, R. König, and E. Jourdain, Rev. Sci. Instrum. **75**, 3268 (2004).
- ⁹E. J. Synakowski *et al.*, Nucl. Fusion **43**, 1653 (2003).
- ¹⁰S. M. Kaye *et al.*, Nucl. Fusion **45**, S168 (2005).
- ¹¹P. Beiersdorfer, M. Bitter, M. J. May, and L. Roquemore, Rev. Sci. Instrum. **74**, 1974 (2003).
- ¹²B. C. Stratton, H. W. Moos, and M. Finkenthal, Astrophys. J. **279**, L31 (1984).
- ¹³P. Beiersdorfer, M. Bitter, S. von Goeler, and K. W. Hill, Nucl. Instrum. Methods Phys. Res. B **43**, 347 (1989).
- ¹⁴B. J. Wargelin, P. Beiersdorfer, D. A. Liedahl, S. M. Kahn, and S. von Goeler, Astrophys. J. **496**, 1031 (1998).
- ¹⁵I. Martinson and C. Jupén, Phys. Scr. **68**, C123 (2003).
- ¹⁶P. Beiersdorfer, M. Bitter, S. von Goeler, and K. W. Hill, Astrophys. J. **610**, 616 (2004).
- ¹⁷J. K. Lepson, P. Beiersdorfer, E. Behar, and S. M. Kahn, Astrophys. J. **590**, 604 (2003).
- ¹⁸S. B. Utter, G. V. Brown, P. Beiersdorfer, E. J. Clothiaux, and N. K. Podder, Rev. Sci. Instrum. **70**, 284 (1999).
- ¹⁹N. Nakano, H. Kuroda, T. Kita, and T. Harada, Appl. Opt. **23**, 2386 (1984).
- ²⁰M.-F. Gu, Astrophys. J. **582**, 1241 (2003).
- ²¹M. Klapisch, A. B. Shalom, J. L. Schwob, B. S. Fraenkel, C. Breton, C. de Michelis, M. Finkenthal, and M. Mattioli, Phys. Lett. **69A**, 34 (1978).